A Recombinant Rabies Virus Expressing the Marburg Virus Glycoprotein is Dependent Upon ADCC for Protection Against Marburg Virus Disease in a Murine Model

Rohan Keshwara[1], Katie R. Hagen[2], Tiago Abreu-Mota[1,3,4], Amy B. Papaneri[5], David Liu[2], Christoph Wirblich[1], Reed F. Johnson[5], and Matthias J. Schnell[1,6*]

[1]Department of Microbiology and Immunology, Sidney Kimmel Medical College at Thomas Jefferson University, Philadelphia, PA, 19107, USA

[2]Integrated Research Facility, National Institute of Allergy and Infectious Diseases, National Institutes of Health, Fort Detrick MD, 21702 USA

[3]Life and Health Sciences Research Institute (ICVS) School of Medicine, University of Minho, 4710-057 Braga, Portugal

[4]ICVS/3B's, PT Government Associate Laboratory, Braga/Guimarães, 4710-057, Portugal

[5]Emerging Viral Pathogens Section, National Institute of Allergy and Infectious Diseases, National Institutes of Health, Bethesda MD, 20892 USA

[6]Jefferson Vaccine Center, Sidney Kimmel Medical College at Thomas Jefferson University, Philadelphia PA, 19107 USA

[*]Corresponding author: Matthias.schnell@jefferson.edu

ABSTRACT Marburg virus (MARV) is a filovirus related to Ebola virus (EBOV) associated with human hemorrhagic disease. Outbreaks are sporadic and severe with a reported case mortality rate upward of 88%. There is currently no antiviral or vaccine available. Given the sporadic nature of outbreaks, vaccines provide the best approach for long-term control of MARV in endemic regions. We have developed an inactivated rabies virus-vectored MARV vaccine (FILORAB3) to protect against Marburg virus disease. Immunogenicity studies in our lab have shown that a Th1-biased seroconversion to both RABV and MARV glycoproteins is beneficial for protection in a preclinical murine model. As such, we adjuvanted FILORAB3 with GLA-SE, a TLR-4 agonist. Across two different BALB/c mouse challenge models, we achieved 92% protection against murine-adapted Marburg virus (ma-MARV). Although our vaccine elicited strong MARV GP antibodies, it did not strongly induce neutralizing antibodies. Through both *in vitro* and *in vivo* approaches, we elucidated a critical role for NK cell-dependent antibody-mediated cellular cytotoxicity (ADCC) in vaccine-induced protection. Overall, these findings demonstrated that FILORAB3 is a promising vaccine candidate for Marburg virus disease.

IMPORTANCE Marburg virus (MARV) is a virus similar to Ebola virus and also causes a hemorrhagic disease, which is highly lethal. In contrast to EBOV, only a few vaccines are developed against MARV and researcher do not understand what kind of immune responses are required to protect from MARV. Here we show that antibodies directed against MARV after application of our vaccine protect in an animal system but fail to neutralize the Virus in widely used virus neutralization assay against MARV. This newly discovered activity needs to be more considered when analyzing MARV vaccines or infections.

INTRODUCTION

Filoviruses are filamentous, enveloped viruses that can cause highly lethal hemorrhagic fever in both humans and nonhuman primates (1). Three major genera comprise the filovirus family: *ebolavirus*, *marburgvirus*, and the newly discovered *cuevavirus*. While the *ebolavirus* genus contains 5 species (*Zaire ebolavirus* [EBOV], *Sudan ebolavirus* [SUDV], *Bundibugyo ebolavirus* [BDBV], *Reston ebolavirus* [RESTV], and *Taï Forest ebolavirus* [TAFV]), the *marburgvirus* genus contains only one, the eponymously named *Marburg marburgvirus* (MARV) (2). MARV is further subdivided based on different isolates, including Ci67, Musoke, and Angola, and the more distinct lineage, Ravn virus (RAVV).

MARV was the first filovirus to be identified when it sickened laboratory workers handling tissue from infected nonhuman primates originating from Uganda in 1967(1). MARV has since re-emerged at least 8 times and has been imported to the United States and Europe by travelers who became infected in Africa (1). MARV Angola subspecies emerged in 2004 and caused the largest MARV outbreak known to date with a case fatality rate of 88%, (3, 4).

The glycoprotein (GP) of filoviruses mediate attachment and entry of the viruses into target cells. In infected cells, GP precursor protein is cleaved during proteolytic transport from the endoplasmic reticulum to the Golgi by host furin protease into two distinct subunits that associate via disulfide bonds (5). In the native MARV GP structure, three monomeric GP1-GP2 pairs come together to form the GP trimer on the viral surface. GP1 is shielded by two heavily glycosylated domains (glycan cap and mucin like domain) which restricts access to the putative receptor binding site and facilitates viral immune evasion by epitope masking (6). GP2 subunit contains part of the mucin like domain, the transmembrane domain to anchor GP into the viral membrane, and the fusion machinery necessary to trigger viral entry into cells (7).

Recent studies in nonhuman primates have demonstrated that passive administration of polyclonal sera against MARV can provide effective post-exposure therapy for MARV infection (8, 9). Monoclonal antibody therapies are also currently being developed for post-exposure prophylaxis (10, 11). However, post-exposure prophylaxis alone is not enough to combat the threat of Marburg Virus Disease (MVD) which may spread quickly once an outbreak has occurred. Preventative treatment with vaccines is strongly needed, especially considering recent ring vaccination methods to strategically limit the spread of Ebola infection (12). Various MARV vaccine approaches are currently underway. MARV GP DNA-based vaccines are safe but have low seroconversion against GP antigen in Phase I clinical trials in humans (13, 14). MARV-VLPs (3 doses plus adjuvant) fully protected cynomolgus macaques against MARV and heterologous Ravn virus (RAVV) lethal aerosol exposure (15). Preclinical work in nonhuman primates using either heterologous multivalent Ad26-Ad35 prime-boost vaccination regimens or vesicular stomatitis virus (VSV) as a platform have shown protection against MARV (range 75%-100% protection) (16-18).

Despite these advances, potential mechanisms of vaccine-induced protection against MARV are still poorly understood, and there is still currently no approved antiviral or vaccine available to treat MARV disease. For a vaccine against MARV to be successful, it should provide long-lasting immunity. Exposures are spontaneous and unpredictable in endemic regions, so long-term immunity in at-risk populations would diminish spillover events to humans from the viral reservoir and could curb subsequent human-to-human transmission to greatly limit the spread of an epidemic. To understand the factors that influence long-term immunity, it is necessary to define the immune response required to achieve prolonged protection against MARV. A recent study reported that MARV survivors develop multivariate CD4+ T cell responses but limited CD8+ T cell responses, suggesting that CD8+ T cell may not be required for a protective response against MARV (19). However, different vaccine platforms may invoke

77 different mechanisms to elicit protection and may not necessarily need to mimic a natural
78 infection (20) . Interestingly, neutralizing antibody responses in MARV survivors are rare and
79 diminish rapidly over time (19, 21).

80 In this study, we evaluated our inactivated bivalent rabies-vectored MARV vaccine,
81 FILORAB3, as a promising human vaccine candidate for Marburg virus, and elucidated the
82 mechanism of protection by determining the parameters of optimal vaccine efficacy. The
83 vaccine is a chemically-deactivated purified rabies virions that expresses and incorporates both
84 RABV G and MARV GP in the virion. We have chosen to use rabies virus (RABV) as our vector
85 for MARV GP for the following reasons: 1) Due to its relative rarity, pre-existing immunity should
86 not be a widespread problem, 2) target populations should be susceptible to successful
87 immunization 3) the RABV vaccine strain used (SAD-B19) is highly attenuated and contains a
88 mutation that abolishes neurovirulence; 4) rabies vaccine vectors replicate efficiently in VERO
89 cells that are qualified for production of vaccines for human use; 5) rabies replicates in the
90 cytoplasm, so integration into the host genome is not a concern, 6) killed rabies virions are
91 replication deficient; 7) recombination events involving the rabies virus genome are extremely
92 rare; 7) insertion of foreign genes into the rabies genome is stable; and 8) The rabies genome
93 only has five genes, and the proteins they encode are not immunosuppressive toward the host
94 (22).

95 Here, we demonstrated in a preclinical murine model that vaccinated animals show Th1-
96 biased seroconversion to both RABV and MARV glycoproteins. Furthermore, when the mice
97 were immunized with a single dose of adjuvanted vaccine, they achieved full protection from
98 lethal challenge with mouse-adapted MARV. Although our vaccine elicited high titers of specific
99 antibodies, there was no strong induction of neutralizing antibodies, even after challenge. As
100 such, we explored the role of antibody-dependent cellular cytotoxicity (ADCC) in protection
101 against MARV challenge. For filoviruses as well as other viruses, neutralization *in vitro* does not

102 necessarily correlate with protection *in vivo*. Non-neutralizing antibodies are known to confer
103 protection by ADCC, phagocytosis, prevention of virus budding, and other mechanisms (10, 23-
104 30). Through both an *in vitro* and *in vivo* approach, we identified an important role for ADCC and
105 other non-neutralizing antibody functions in vaccine-induced immunity by FILORAB3.

106

107

RESULTS

Generation of a rabies vaccine encoding a Marburg virus GP. Recombinant rabies virus expressing MARV glycoprotein (i.e., FILORAB3) was constructed by inserting a gene composed of rabies transcriptional start and stop sequences flanking the codon-optimized MARV Angola strain GP in between the nucleoprotein (N) and phosphoprotein (P) genes of BSNP333, an attenuated parental rabies vector derived from the SAD B19 vaccine strain (31-34). Based on our previous studies showing that codon-optimization can increase the level of foreign glycoprotein expression and incorporation into budding rabies virions (35, 36), we utilized a codon-optimized version of MARV GP (Angola strain). The vector BNSP333 also contains an arginine to glutamine mutation in amino acid position 333 of the rabies glycoprotein, which further reduces neurovirulence and thus increases its safety profile (37). For our studies, we generated both live, replication-competent and chemically-inactivated versions of the recombinant virus (Fig. 1). FILORAB3 was inactivated by treatment with beta-propriolactone, an alkylating agent frequently used to inactivate viruses including RABV (38).

Infectious recombinant virus was recovered by transfecting into BSR mammalian cells the FILORAB3 cDNA along with support plasmids individually bearing each of the RABV genes under the control of a T7 promoter and a plasmid-expressing T7 polymerase, as previously described (7, 37). To evaluate the *in vitro* replication potential of live FILORAB3, BSR cells were infected in a multi-step growth curve at a multiplicity of infection of 0.1 with the initial passages of recovered live virus in parallel with the parental vector, BNSP333, and previously developed recombinant rabies virus bearing the Ebola glycoprotein Mayinga strain (i.e., FILORAB1) (Fig. 2). Viral titers were assessed at several timepoints for a duration of 96 h post-infection. While the appearance of viral progeny was not different between the parental strain and recombinant virus, FILORAB3 did grow to a lower overall titer by the terminal timepoint of 96 h post-infection, similar to FILORAB1.

Expression of MARV GP by recombinant RABV vaccine. To confirm efficient co-expression of both the RABV and MARV glycoproteins in cells infected with recombinant virus, VERO cells were infected at an MOI of 0.1 with either live FILORAB3 or BNSP333 (control) for 48 h before immunofluorescence surface staining was performed. Monoclonal antibodies directed against RABV G appear in green, monoclonal antibodies directed against MARV GP appear in red, and overlap of expression of both glycoproteins is indicated by yellow (Fig. 3A). Cells that were infected with FILORAB3 recombinant virus exhibited co-expression of both glycoproteins, which suggests that these envelope proteins are being properly expressed by the vaccine vector, folded, and trafficked to the surface.

Incorporation of MARV GP into RABV virions. For the inactivated vaccine to be immunogenic against both RABV G and MARV GP, both glycoproteins must be incorporated into budding virions. To analyze the incorporation of RABV G and MARV GP into purified virions, virus particles were isolated from the supernatant of infected VERO cells by filtration and concentration followed by purification over a 20% sucrose cushion. The virus particles were resolved by SDS-PAGE and visualized by SYPRO Ruby staining. FILORAB3 purified virions showed incorporation of all essential RABV proteins (Fig. 3B, left image) and in the same ratios as the parental virions (lane 3 vs. lane 1). An additional protein of the expected size for MARV GP1 (170 kDa) was detected in FILORAB3 viral particles (highlighted in the red box) (5, 39, 40). GP2 cannot be visualized on this gel because it migrates at a similar size as the RABV P protein. FILORAB1 was included as a positive control. Incorporation of the codon-optimized MARV GP appears to occur but a to a lesser extent than previously shown for EBOV GP.

To confirm expression of both subunits of MARV glycoprotein, we analyzed purified virions by Western blot (Fig. 3B, right image) and probed with a cocktail of two monoclonal antibodies directed against both GP1 and GP2. Two proteins migrating at about 170 kDa and 40 kDa, consistent with the molecular weight of MARV GP1 and GP2, were detected (39, 40) (Fig.

158 3B, lane 3). These results further confirm that MARV GP has been incorporated into the virion
159 and has been cleaved and processed. Two proteins of similar size were detected in cell lysates
160 from VERO E6 cells infected with wildtype MARV (lane 5). No protein was detected in mock-
161 infected VERO E6 cell lysates (lane 6) or in lysate from cells infected with an unrelated virus
162 (Lassa virus, lane 7), indicating that the identified bands are in fact specific to FILORAB3 and
163 Marburg protein incorporation.

164 **Pathogenicity in vivo.** We know from previous studies in our lab that BNSP333 is apathogenic
165 in adult mice but neurovirulent in suckling mice following intracranial (IC) inoculation (41). To
166 assess whether inclusion of MARV GP into the BNSP333 vector would increase neurovirulence,
167 newborn/suckling mice were IC inoculated with escalating doses of FILORAB3 (Fig. 4A). As a
168 positive control, we used BNSP vector which lacks the attenuating mutation at amino acid
169 position 333 in RABV G. Mice receiving FILORAB3 experienced significantly delayed lethality
170 compared to control mice ($p<0.0001$). The majority of mice in each FILORAB3 group ($\geq$70%)
171 survived up to at least day 10 compared to control mice which all succumbed to infection by day
172 5. with the majority surviving up to day 10 post challenge versus total lethality for all control mice
173 by day 5. This suggests that FILORAB3-infected mice retained the neurovirulence characteristic
174 of the parental BNSP333 vector but did not exacerbate it (Fig. 4A). To further evaluate safety of
175 the vaccine, we exposed adult severe combined immunodeficient (SCID) mice to FILORAB3 or
176 BNSP by intramuscular injection in the thigh of $6\log_{10}$ FFU (Fig. 4B) (42). As expected, the
177 control mice all succumbed by day 20 post-infection while the mice receiving FILORAB3 all
178 survived, further demonstrating the safety of FILORAB3. Taken together, these data indicate
179 that FILORAB3 possesses a good safety profile for use as a live vaccine in certain target
180 species. Furthermore, the inactivated FILORAB3 vaccine for humans should be even safer
181 since it does not have the capacity to replicate.

FILORAB3 induces humoral immunity to both RABV and MARV in mice. To analyze the immunogenicity of FILORAB3, groups of 5 C57BL/6 mice were immunized with 2 intramuscular doses, 28 days apart, of either inactivated FILORAB3 plus adjuvant or the parental control vaccine (BNSP333) plus adjuvant (Fig. 6A). Previous studies in NHPs with FILORAB1 indicated that a TLR-4 agonist, glucopyranosyl lipid adjuvant (GLA) in a squalene-in-water emulsion (GLA-SE), not only increases the humoral responses but also stimulates a Th1-biased humoral immune response that is considered beneficial for viral infection and protection against EBOV by RABV-based vectors (43). Therefore, we also included GLA-SE in our preclinical studies with FILORAB3 (44). Furthermore, GLA-SE has been shown to enhance the breadth and quality of humoral immune responses for influenza virus (35, 45-49).

We collected final sera from the mice 42 days after the initial immunization and characterized the sera in indirect ELISA with soluble MARV GP (Fig. 5). Mice immunized with FILORAB3 plus adjuvant showed robust seroconversion towards MARV GP while GP-specific titers were not detected in negative controls (i.e., vector immunized mice). Both control and FILORAB3-immunized groups of mice showed strong seroconversion toward RABV G (Figs. 6B and C). To confirm a Th1-biased humoral response, we analyzed the isotype-specific antibody response by ELISA in mice receiving adjuvanted inactivated FILORAB3. Based on the relative titers of IgG2c to IgG1 in FILORAB3-immunized mice, it appears that the immune response is biased toward production of Th1 antibodies (Fig. 6D).

Neutralizing antibodies against MARV are not induced by FILORAB3 immunization. Based on the high titers of MARV GP-specific antibodies elicited by our vaccine in mice, we tested whether these antibodies had the capacity to neutralize *in vitro*, thereby illuminating a potential mechanism of protection. To this end, we employed the use of a lentiviral pseudotyped virus expressing a luciferase reporter gene (50, 51). The assay was performed with purified immunoglobulin G (IgG) derived from the final sera of mice in the previously described

immunization study and virus neutralization percentage was standardized from the relative luminescence units readout. Compared to a positive control antibody (gray line) known to neutralize both retroviral and VSV pseudotypes containing MARV GP *in vitro* (52), purified IgG from the sera of FILORAB3-immunized mice did not elicit any detectable titers of neutralizing antibodies which were comparable to levels detected in sera from negative control mice (i.e., background) (Fig. 6E, top panel). By contrast, both groups of sera elicited robust titers of RABV neutralizing antibodies (compared to a positive control human mAb, gray line), which is a known correlate of protection against rabies virus (49, 53-55).

FILORAB3 confers protection against ma-MARV challenge in mice (in the absence of neutralizing antibodies). After we established that mice immunized with adjuvanted FILORAB3 had high titers of MARV GP-specific antibodies but insignificant titers of neutralizing antibodies, we analyzed the potential to protect mice against lethal challenge with the mouse-adapted Marburg virus (ma-MARV). Groups of 10 BALB/c mice with equally split gender were immunized with either 1, 2, or 3 doses of adjuvanted FILORAB3 vaccine, according to the schedule defined in Fig. 7A (Groups 5-7). One group of mice also received a single inoculation of live, replication-competent FILORAB3 (Group 4), and another group received live, replication-competent BNSP333 as a negative control for the live virus vaccination (Group 3). To assess survival throughout the course of the experiment, we included vehicle-infected mice that did not receive any challenge (Group 1). As a positive control for lethality by ma-MARV, we included a group immunized with vehicle and challenged with a lethal dose of ma-MARV (Group 2).

Whereas all negative control vaccine groups (Groups 1-3) as well as mice immunized with live FILORAB3 (Group 4) succumbed to the infection by day 7 after challenge, we were able to achieve full protection against lethal ma-MARV challenge with just one inoculation of adjuvanted FILORAB3 (Fig. 7B). Linear regression analysis of the average OD490 nm value at the lowest antibody dilution (1:50) versus the percent of survival for each group revealed that

antibody titers correlated with survival (r^2 = 0.7945). Analysis of pre-challenge sera (from D-40) from these groups of mice by ELISA revealed that GP-specific seroconversion was achieved in all groups immunized with adjuvanted inactivated FILORAB3. Moreover, these titers were high compared to background (Fig. 7C). Administering 2 and 3 doses of FILORAB3 increased the GP-specific titer in a dose-dependent fashion.

Mice immunized with live FILORAB3 (red line) seroconverted to MARV GP, but the GP ELISA titers were much lower compared to the inactivated vaccine groups. Live FILORAB3 immunized mice were fully susceptible to challenge, thereby suggesting that immunogenicity from GP expression by the live, replication-competent vaccine is not able to control infection from ma-MARV, despite eliciting Th1-biased GP-specific antibodies. Thus, these data suggest that it is not solely elicitation of a Th1-type response that informs vaccine-induced survival, but also, a threshold antibody response must be achieved. We have encountered this phenomenon in our previous vaccine study with FILORAB1 in NHPs. One protected NHP had a clear Th2-biased humoral response but was still protected against lethal challenge, presumably due to high pre-challenge antibody titers (56).

As expected, all mice receiving either live or inactivated vaccine seroconverted toward RABV G in a dose-dependent manner for the inactivated vaccine groups (Fig. 7C, right panel). Th1 bias of the humoral response was confirmed as measured by isotype ELISAs comparing the ratio of IgG2a to IgG1 at the lowest sera dilution (1:150) in these BALB/c mice (Fig. 7D). Post-challenge GP- and G-specific antibody titers in mice that survived ma-MARV challenge remained high, and GP-specific antibody titers increased in mice receiving 1, 2, or 3 doses of adjuvanted vaccine after challenge as measured by EC50 values, indicating that vaccine-induced immunity can confer protection by controlling viral infection (Fig. 7E). Th1 skewing of the humoral response is maintained after challenge in survivors, as measured by isotype

ELISAs comparing the ratio of IgG2a to IgG1 at the lowest sera dilution (1:450) (Fig. 7F). This suggests that a Th1-bias is important for a survival response toward MARV.

We also assessed the MARV and RABV neutralizing antibody titers in pooled sera samples both pre- and post-challenge in mice in this study. Consistent with the results of the immunogenicity study previously described in C57BL/6 mice, BALB/c mice in this study immunized with either live or inactivated FILORAB3 did not elicit neutralizing antibody titers against MARV GP (Fig. 7G, top panels). In contrast, all mice receiving either live or inactivated FILORAB3 did elicit potent neutralizing antibodies against RABV G pre- and post-challenge, and the effect seemed to be dose-dependent: the groups of mice receiving 2 and 3 doses of adjuvanted vaccine elicited increasingly higher titers of RABV G-specific nAbs (Fig. 7G, bottom panel).

Antibody Dependent Cellular Cytotoxicity. Based on the strong immunogenicity of FILORAB3 against both RABV G and MARV GP, negligible titers of neutralizing antibodies against MARV GP, and survival in mice following challenge with ma-MARV, we hypothesized that non-neutralizing antibodies might be important for vaccine-induced protection. To assess the capacity of antibodies elicited by vaccination to participate in ADCC effector functions, we developed an *in vitro* flow-based ADCC assay (Fig. 8). Briefly (as demonstrated in Fig. 9A), mouse 3T3 fibroblast target cells were transduced with mouse retrovirus expressing both an EGFP reporter gene and MARV GP gene. These target cells were confirmed to express MARV GP on their surface by flow cytometry (Fig. 9B). Target cells were then incubated with 50ug/mL of purified IgG derived from sera from immunized mice before the addition of primary effector NK cells purified from splenocytes from naïve mice (Fig. 9C). After 4 h, the population of dead target cells over the total population of target cells was assessed and reported as the percent of cytotoxicity (Fig. 9D).

At an effector to target cell ratio of 5:1, antibodies from mice immunized with adjuvanted, inactivated FILORAB3 demonstrated significantly more specific killing of target cells expressing MARV GP ($p < 0.0001$) than negative control sera from BNSP333-immunized mice (Fig. 8). Furthermore, blocking the Fcγ receptor on the surface of NK cells abrogated the NK-cell mediated cytotoxicity to background killing levels, indicating that killing by NK cells in this assay is enhanced by GP-specific antibodies binding to the receptor and activating NK cells. While similar findings have been demonstrated with Ebola GP-specific NHP (25), this result adds to the growing body of evidence suggesting that non-neutralizing antibodies may be important for controlling MARV infection (57).

FcyR receptor is important for in vivo protection in mice. To test the *in vivo* relevance of Fc receptor-dependent effector mechanisms to confer protection, we utilized a Fc-gamma chain knockout mouse model (43, 58, 59). This model has normal B and T cell compartments but does not express FcR1, II, III, or IV receptors on the surface of immune effector cells (i.e., macrophages, monocytes, NK cells) (43, 58, 59). Either wildtype BALB/c or FcyKO mice (on BALB/c strain background) were immunized with 1 or 2 doses of adjuvanted FILORAB3 vaccine (Groups 5-8). As positive controls, one group of WT mice and one group of KO mice (Groups 2 and 4) were mock immunized before challenge. As a study control, we included WT and KO mice that were immunized with vehicle but remained unchallenged. Each group consisted of 12 mice total (6 male and 6 female) (Fig. 10A).

Wildtype mice receiving 1 dose of adjuvanted vaccine demonstrated significantly better survival compared to FcγKO mice receiving 1 dose of adjuvanted vaccine (58.3% protection vs. 0% protection, $p = 0.0058$) (Fig. 10B). To confirm that the difference in survival was not due to differential GP-specific antibody titers, we performed ELISA on pre-challenge sera from these mice (D-40). We did not see a significant difference in either RABV G or MARV GP-specific titers between these groups ($p > 0.9999$) (Fig. 10C). Survivors of challenge demonstrated an

increase in GP-specific antibody titers with no significant differences between the indicated groups (Fig. 10D). When we assayed for neutralizing antibodies *in vitro*, we found that neither of the single dose groups elicited detectable titers of neutralizing antibodies (Fig. 10E, top left panel), findings that suggested that differences in their survival are tied to the lack of functional Fc receptors in the KO group. In WT and KO mice receiving 2 doses of the vaccine, serology testing by ELISA confirms that pre-challenge sera (D-40) titers of RABV G and MARV GP are not significantly different ($p > 0.9999$) (Fig. 10C), and there is no significant difference in survival between these groups ($p > 0.9999$) Fig. 10B). The neutralizing antibody response elicited by both WT and KO mice receiving 2 doses of FILORAB3 was low, with greater than 50% reduction in infection achieved only at the lowest dilution of antibody (1:10), although the effect was insignificant considering variability (standard deviation of mean) (Fig. 10E). While we expected survival in the wildtype group, it was interesting that the 2-dose KO group showed survival. While the presence of a low titer of neutralizing antibodies in these groups could possibly have provided some protection against ma-MARV in the absence of Fc receptor function by limiting the spread of the virus, it was unlikely, since these GP-specific antibody titers were very low and our *in vitro* assay overestimates neutralizing antibody titers compared to the wildtype virus (50-52). Therefore, it is likely that other Fcγ-independent antibody effector mechanisms are involved in vaccine-induced immunity and protection, but it is clear from the results of this study that Fc gamma receptor mechanisms have an important role in vaccine-induced protection.

DISCUSSION

We have described the generation, propagation, safety, immunogenicity, and protective efficacy of an inactivated recombinant rabies vectored Marburg virus vaccine, FILORAB3, developed by successful incorporation of the codon-optimized version of Marburg GP into RABV virions expressing native RABV G. Our results demonstrate that FILORAB3 induced strong humoral immunity in mice, as indicated by high titers of Th1-biased antibodies against MARV glycoprotein but negligible titers of MARV neutralizing antibodies. The antibody response against MARV is consistent with features of natural Marburg virus infection in both humans and NHPs, whereby survivors experience Th1 skewing of the humoral response marked by the rare occurrence of neutralizing antibodies that decrease rapidly over time (19, 21).

Based on its robust immunogenicity *in vivo*, we sought to evaluate the efficacy of FILORAB3 in a murine challenge model. From our previous immunogenicity and challenge studies in mice and NHPs with the recombinant RABV/Ebola virus vaccine candidate (FILORAB1), it was apparent that the quality of the antibody response has important consequences on protection elicited by our vaccine (56). As such, we chose to adjuvant FILORAB3 with GLA-SE (35, 46-48) with the goal of recapitulating a Th1- biased effect on the immune response. Two doses of the adjuvanted vaccine conferred 96% survival (combined efficacy from 2 challenge experiments) in mice against mouse-adapted MARV while unprotected mice succumbed to the infection by day 7. Differences in survival between single-dose immunized mice in the first and second mouse challenge study could be due to apparent differences in threshold of the antibody response. Matrajt *et al.* used modeling to show that above a certain response threshold, vaccinating more people with one dose of the influenza vaccine resulted in lower attack rates. However, below that required level of response, vaccinating fewer people with 2 doses is better for protection (60). A single dose of our FILORAB3 vaccine elicits a more variable response in the population, likely reflective of

relatively small number of subjects. After a single dose vaccination, some animals are above threshold, and some are below the required threshold for protection. Varicella zoster virus (VZV) vaccine shows 94.9% seroconversion after a single dose but only 100% after 2 doses (61). In a pre-exposure setting, immunization with the human rabies vaccine must reach a threshold of at least 0.5 international units per mL of neutralizing activity in order to be protective. To achieve this protective threshold in 100% of the population, at least 3 doses of the rabies vaccine must be given (62). In our preclinical models, 2 doses of our FILORAB3 vaccine give uniform results across both studies. Overall, 2 immunizations of vaccine may achieve higher variation in the epitope specificities of GP-specific antibodies (63), which can have positive implications for long-lasting immunity.

Pre-challenge levels of antibody in mice immunized with inactivated vaccine were similar to levels observed after challenge, indicating that vaccination established and maintained a crucial memory B-cell response. Mice receiving a single inoculation of the live FILORAB3 had low titers of GP-specific antibodies and were not protected against lethal challenge, suggesting that antibodies play a major role in protection. Live virus vaccine antigenicity is dependent upon replication of the virus. It is possible that the live virus is highly attenuated upon peripheral administration and the antigen load is not enough to induce a protective response. It is also possible that the immune response mounted against RABV G might quickly block the spread of the vector (at least in intramuscular immunization) and therefore prevent a potent IgG immune response against MARV GP. This is corroborated by our data which show that the RABV G immune response with live FILORAB3 is lower than the corresponding response with killed vaccine. Furthermore, live attenuated viral vectors encoding foreign glycoprotein are known to induce potent cellular immune responses because they engage the endogenous pathway or cross-priming to present epitopes via MHC I to CD8+ T cells (64, 65). Since live FILORAB3 does not confer protection in mice, it suggests that cytotoxic T cells may not play a major role in

vaccine-induced protection against MARV or at least are not sufficient to control MARV infection in the absence of an appropriate antibody response.

In pursuit of defining antibody-mediated mechanisms of protection by FILORAB3, we concluded that neutralizing antibodies do not play a significant role in protection against survival. However, since we see high titers of specific IgG after vaccination, we hypothesized that non-neutralizing antibodies are involved in protection. This hypothesis was also supported by the finding the antibody levels correlated to survival ($r^2 = 0.7945$). Functions of non-neutralizing antibodies have been described for other viruses. We know that cocktail of exclusively non-neutralizing antibodies can protect NHPs against lethal Ebola challenge when administered as post-exposure prophylaxis (66). ZMapp, first used in the West African Ebola outbreak as emergency post-exposure prophylaxis, was developed to include a non-neutralizing antibody (c13C6) that binds to the tip of the viral glycoprotein after it was shown that inclusion of this antibody resulted in better survival in guinea pigs and in NHPs than a cocktail of neutralizing antibodies only (67). Non-neutralizing antibodies to HIV and lymphocytic choriomeningitis virus GPs inhibit infection of DCs and of macrophages and limit virus spread (66, 68). Various non-neutralizing functions of antibodies elicited by vaccination against HIV have been described previously in great detail (44, 69, 70), and the recent RV144 Thai vaccine trial showed a correlation of protection between non-neutralizing antibodies and protection (71, 72).

To this end, we developed a novel, *in vitro* flow cytometry-based mouse ADCC assay to assess the ability of antibodies elicited by FILORAB3 to induce direct killing by NK cells (23). Purified IgG from the sera of mice immunized with 2 doses of adjuvanted FILORAB3 led to a significantly higher levels of killing by NK cells compared to purified IgG from sera of mice immunized with parental rabies vaccine alone plus adjuvant. When either GP-specific or control antibodies alone or NK cells alone were added to target cells expressing MARV GP, killing was significantly lower than when both specific antibodies and NK cells were present in the system.

Furthermore, the cytotoxic effect could be abrogated to background levels of killing by the addition of mouse-specific FcγRIII-blocking antibodies. Taken together, these data demonstrate that NK cell-mediated killing measured in this assay is dependent upon FcγRIII receptor engagement with GP-specific antibodies. Furthermore, killing is antigen-dependent as GP-specific antibodies did not enhance killing beyond a background level for both target cells expressing either a different viral glycoprotein (Lassa virus GPC) or no viral envelope (Fig. 9E). While the importance of Fc gamma-dependent antibody-mediated immune responses have been described for Ebola virus (24-26), this result provides the first piece of evidence that ADCC may play a significant role in the protection against Marburg virus (24, 73). Other Fcγ-dependent mechanisms of protection, such as FcγRI receptor-mediated phagocytosis or killing by macrophages or monocytes, could also be important and have been described in viral immunity for other viruses but were not tested within the scope of this study (28-30).

For filoviruses, *in vitro* ADCC capacity is not necessarily an effective predictor of *in vivo* protection (10). Therefore, we sought to determine the *in vivo* relevance of Fcγ-dependent antibody-mediated mechanisms of protection in a knockout mouse model in the BALB/c background. These knockout mice were developed by embryonic gene targeting to replace the gamma chain gene with a null allele. As a result, among other gamma chain-dependent immune effector functions, these mice have NK cells that lack ADCC function but are fertile and viable and have normal B and T cell compartments (43). We found no significant difference in the titers of GP-specific antibody induced between wildtype and KO mice receiving one dose of adjuvanted vaccine, but there was a significant difference in the survival between these groups. Since both pre-challenge animals and survivors had negligible titers of GP neutralizing antibodies (consistent with previous *in vitro* murine models), we concluded that in the absence of these potently neutralizing antibodies, functional Fcγ receptor is essential for survival in these mice. However, since KO mice receiving 2 doses of the vaccine showed indiscriminate survival

426 from the corresponding WT group, then it is apparent that Fcγ-independent mechanisms of
427 protection are also involved in protection. Takada *et al*. described *in vitro* the phenomenon of
428 GP specific antibodies that participate in budding inhibition of MARV. These antibodies are not
429 classically neutralizing but can bind to GP on the surface of infected cells and prevent budding
430 of progeny virions (57). Non-neutralizing antibodies that fix complement can also be an
431 essential part of the antibody repertoire induced by FILORAB3 vaccination. The classical
432 complement pathway has been shown to impact the control of influenza virus infections (74-77)
433 and has been shown to be able to directly lyse HIV virions (78, 79). It is possible that our
434 vaccine elicits antibodies that could bind to GP on the surface of infected cells and recruit C1q
435 protein to initiate the classical complement cascade to lyse the infected cell or mediate
436 opsonophagocytosis, however, complement added to our *in vitro* neutralization study does not
437 decrease infectivity of lentivirus pseudotyped virions (data not shown), so direct lysis of MARV
438 virions is not a likely mechanism of action. Lastly, since our vaccine is adjuvanted with GLA-SE,
439 which is known to elicit type II interferon responses by induction of neutrophils and CD8+ T cells
440 (80, 81), the possibility cannot be excluded that vaccination elicits CTLs that can kill virally
441 infected cells during acute infection.

442 The studies described here demonstrate the potential for a RABV platform for the
443 development of a safe and effective MARV vaccine. We have demonstrated preclinical safety
444 and efficacy against the Angola strain of ma-MARV in mice. While protection against the highly
445 pathogenic Angola strain is thought to confer protection against other MARV strains and RAVN
446 (82-87), this still needs to be assessed with FILORAB3 in animal models. Presently, the
447 immunogenicity and protective efficacy of FILORAB3 needs to be evaluated in NHPs to
448 determine whether this candidate vaccine merits evaluation in humans, but preclinical results in
449 mice, described in this paper, offer a promising outlook for the development of a human
450 FILORAB3 vaccine. Additionally, further investigation into various other mechanisms of

451 protection are warranted in order to understand the optimal parameters of long-lasting immunity
452 by FILORAB3.

453

Materials and Methods

cDNA construction of vaccine vectors.

We inserted codon-optimized Marburg virus glycoprotein gene GP (Angola strain, GenBank: KY047763.1) in between the N and P genes of the parental BNSP333 rabies vector using BsiWI and NheI restriction sites. Codon bias optimization for human codon use was carried out by GenScript, Inc. The resulting plasmid was designated BNSP333-coMARV-GP (FILORAB3), and the correct sequence of the plasmid was confirmed by sequencing using primers targeting the region between the N and P genes.

Recovery of recombinant vectors.

X-tremeGENE 9 transfection reagent (Roche Diagnostics) in Opti-MEM was used to transfect full-length viral cDNA clones along with support plasmids bearing RABV N, P, G, and L genes under the control of a T7 promoter and a plasmid expressing T7 RNA polymerase into BSR cells on 6-well plates as described previously (32-34). Successful recovery was determined by a rabies focus-forming assay. Briefly, 7 days after transfection, supernatant from each transfected well of the 6-well plate was transferred to duplicate wells of a 12-well plate seeded with VERO cells. 48 h later, cells in the 12-well plate were fixed with 80% acetone and stained with a FITC-conjugated antibody against RABV N (Fujirebio Diagnostics, Inc). Fluorescence microscopy was used to observe the appearance of viral foci, indicative of recovered, infectious recombinant RABV.

Sucrose purification and inactivation of the virus particles.

FILORAB3 was grown large-scale by infecting VERO cells in a 2-stack plate at MOI = 0.001. The supernatant was collected every 4 days for a total of 6 harvests. Harvests were titered using rabies focus-forming assay and harvest 4-6 were pooled and concentrated 9x in a stirred 300-ml ultrafiltration cell (Millipore). Concentrated supernatant was then centrifuged for 2 h at 25,000 rpm through a 20% sucrose cushion using SW32 Ti rotor (Beckman, Inc.) to pellet virus particles. Virion pellets were resuspended in phosphate-buffered saline (PBS), and protein concentrations were determined using a bicinchoninic acid (BCA) assay kit (Pierce). The virus particles were chemically inactivated with β-propiolactone (BPL) at a dilution of 1:2000 overnight at 4 °C. BPL in the virus preparation was inactivated the next day by hydrolysis at 37 °C for 30 min. The absence of infectious particles was verified by inoculating VERO cells in a T25 vessel with 10 µg of BPL-inactivated virus for 2 passages. Inoculated cells were fixed and stained with FITC-conjugated anti-RABV N mAb and visualized by fluorescence microscopy for the presence of foci of infection.

Immunofluorescence testing of the vaccine.

VERO cells were plated onto 12-well plates with 3E5 cells with 15mm circular diameter coverslips inserted and then incubated overnight at 37 °C. The next day the wells were infected at an MOI of 0.01 in 500 µL of serum-free media (OptiPro) per well with FILORAB3 or BNSP333, mixed by rocking, and then incubated at 34 °C for 48 h. After 48 h, cells were washed with one mL of 1x PBS, then fixed with 500 µL of 2% paraformaldehyde (PFA) diluted in PBS for 15 min at room temperature. PFA was removed by aspiration and cells washed 3x with 1x PBS. 1 mL of blocking solution (4% fetal bovine serum [FBS] in PBS) was added to each well for 1 h at room temperature while on the shaker. Blocking solution was aspirated off, then 500 µL of primary antibody diluted 1:250 in 2% FBS was added for 1 h while rocking. Cells were

washed 4 times with 1x PBS and then 500 µL of 1:300 secondary antibodies containing Cy2 and Cy3 dyes and incubated at room temperature for 45 min. Cells were washed 5 times with 1x PBS and then cells were mounted onto slides with the mounting solution containing DAPI with the coverslips face down onto the slide and stored overnight at room temperature for viewing the next day.

Pathogenicity and immunogenicity studies.

(i) Animal ethics statement

This study was carried out in strict adherence to recommendations described in the Guide for the Care and Use of Laboratory Animals (15), as well as guidelines of the National Institutes of Health, the Office of Animal Welfare, and the United States Department of Agriculture. All animal work was approved by the Institutional Animal Care and Use Committee (IACUC) at Thomas Jefferson University (animal protocols 00990, 01155, 01647). All procedures were carried out under isoflurane anesthesia by trained personnel, under the supervision of veterinary staff. Mice were housed in cages, in groups of 5, under controlled conditions of humidity, temperature, and light (12-h light/12-h dark cycles). Food and water were available ad libitum.

ii) Immunizations

Two groups of 6- to 8-week old C56BL/6 mice were immunized intramuscularly with 10 µg of virus particles and 5 ug of GLA-SE in a total volume of 100 µL (50 µL per hindlimb). The 2 groups were as follows: inactivated FILORAB3 and inactivated BNSP333. Each group consisted of 5 female mice. Mice receiving inactivated vaccine were given 2 doses on day 0 and day 28.

iii) Pathogenicity experiments

Groups of suckling mice (n=8) were intracranially infected with escalating doses of FILORAB3 (2 log_{10}, 4 log_{10}, 5 log_{10} ffu) or 5log_{10} FFU of parental rabies, BNSP. Groups of adult SCID mice (n=8) were intracranially infected with 6 log_{10} ffu of live FILORAB3 or parental rabies, BNSP. The mice were monitored for signs of disease such as ruffled fur, ataxia, and disorientation and weighed until day 40. Mice that lost more than 20% of their original weight were considered to have reached the endpoint and were euthanized.

All vaccine efficacy experiments involving the use of mouse-adapted MARV (GenBank Accession number KM261523) were performed under Bio Safety Level-4 conditions at the National Institute for Allergy and Infectious Disease Integrated Research Facility-Frederick MD and approved by the National Institute for Allergy and Infectious Disease, Division of Clinical Research, Animal Care and Use Committee. Samples removed from the BSL-4 environment for further analyses were inactivated by 5MRad gamma-irradiation (sera) or Trizol LS in a 3:1 vol:vol ratio (whole blood). Seven groups of 10 mice each were vaccinated as follows: Group 1: Vehicle (PBS)-no ma-MARV exposure, Group 2: Vehicle (PBS), Group 3: BNSP333 (rabies parental vaccine virus) 5.69 log10 PFU of vaccine, Group 4 FILORAB3, 5.69log10 PFU of vaccine, Group 5: 10µg inactivated FILORAB3 + 5µg GLA-SE D-40 vaccination, Group 6: 10µg inactivated FILORAB3 + 5µg GLA-SE D-54, D-40 vaccination (prime-boost). Group 7: 10µg inactivated FILORAB3 + 5µg GLA-SE D-61, D-54, D-40 vaccination (prime-boost-boost). All groups except Group 1 were exposed to 1,000 PFU ma-MARV by intraperitoneal injection and Group 1 received PBS on D0.

Production of HA-tagged MARV-GP.

Subconfluent T175 flasks of 293T cells (human kidney cell line) were transfected with a eukaryotic expression vector (pDisplay) encoding amino acids 1 to 643 of the head and stalk domains of codon-optimized MARV-GP (Angola strain) fused to a C-terminal hemagglutinin (HA) peptide. Supernatant was collected 48 h after transfection, clarified by centrifugation, and filtered through a 0.45 um filter before being loaded onto an equilibrated anti-HA agarose column (Pierce) containing a 2.5 ml agarose bed volume. The supernatant was allowed to bind to the column overnight at 4 °C. The next day, the column was washed with 10-bed volumes of TBST (TBS with 0.05% Tween 20) and 2-bed volumes of TBS, and bound MARV-GP-HA was eluted with 5 ml of 250 ug/ml HA peptide in TBS. Fractions were collected and analyzed for the presence of coMARV-GP by Western blotting with monoclonal anti-HA antibody (Sigma) prepared in 5% BSA-TBST. Peak fractions were pooled and dialyzed against PBS in 10,000 molecular weight cutoff dialysis cassettes (MWCO) (Thermo Scientific) to remove excess HA peptide. After dialysis, the protein was quantified by BCA and frozen in aliquots at -80 °C. Further characterization was carried out by Western blotting analysis with monoclonal mouse antibodies 3E10 and 5A2 to confirm presence of both GP1 and GP2 subunits, respectively.

RABV and MARV-GP Response by ELISA.

Sera from immunized mice were collected by retro-orbital eye bleed under isoflurane anesthesia on days 0, 28, and 42, and samples were tested for immunogenicity by indirect ELISA using C-terminus HA-tagged soluble recombinant protein for antibody capture (Fig. 5). We tested individual mouse sera as well as purified immunoglobulin G from day 42 for the presence of total IgG specific to MARV-GP and RABV-G. To test for anti-MARV-GP humoral responses, we produced soluble MARV GP (sMGP) as described above. Soluble MARV GP was resuspended in coating buffer (50 mM Na2CO3 [pH 9.6]) at a concentration of 0.5 ug/mL and then plated in 96-well ELISA MaxiSorp plates (Nunc) at 100 µL in each well. RABV-G was also resuspended in coating buffer at a concentration of 0.5 ug/mL and then plated in 96-well ELISA MaxiSorp

plates (Nunc) at 100 µl per well. After overnight incubation at 4 °C, plates were washed 3 times with PBST (0.05% Tween 20 in 1× PBS) and incubated for 1 h at room temperature with blocking buffer (5% dry milk powder in 1x PBST) in a volume of 250 µl per well. The plates were then washed 3 times with PBST and incubated overnight at 4 °C with 3-fold or 4-fold serial dilutions of sera from immunized mice in PBS containing 0.5% BSA. Plates were washed 3 times the next day, followed by the addition of horseradish peroxidase-conjugated goat anti-mouse-IgG (H+L) secondary antibody (1:20,000) (Jackson ImmunoResearch). After incubation for 2 h at room temperature, plates were washed 3 times with PBST, and 200µl of o-phenylenediamine dihydrochloride (OPD) substrate (Sigma) was added to each well. The reaction was stopped by the addition of 50 µl of 3 M H_2SO_4per well after 15 min. Optical density was determined at 490 nm (OD490).

Antibody-dependent cellular cytotoxicity (ADCC).

In the direct ADCC assay, target cells were 3T3 mouse fibroblast cells made to express GP antigen on their surface by transduction with murine stem cell virus bearing the GP gene (MSCV-MARV GP) and GFP reporter gene. Effector cells were primary NK cells derived from naïve mouse splenocytes and purified by Miltenyi MACS® Mouse NK cell isolation kit II. Purified NK cells were further enriched in culture with recombinant mouse IL-2 and IL-15 cytokines.

Procedurally, labeled target cells were seeded in a 96-well U-bottom plate and incubated for 30 min at 37 °C with 50ug/mL of purified IgG derived from sera from animals previously immunized with FILORAB3 to allow binding of GP-specific antibodies to surface antigen. Non-specific sera were used as negative controls. Subsequently, purified NK cells were added at an effector cell-to-target cell ratio of either 5:1 or 10:1 and incubated for 4 h at 37 °C. Propidium iodide (35ug/mL) viability dye was then added to these cells which were analyzed by flow cytometry

using a BD LSR-Fortessa cytometer. ADCC activity was measured as the percent of target cells killed (GFP/PI positive) out of the total GFP positive target cell population (1).

Virus neutralization Assay (VNA).

HIV lentivirus bearing a luciferase reporter gene was pseudotyped with either MARV GP or RABV G and 10,000 infectious particles per well (as measured by qPCR using ABM® lentiviral tittering assay) were incubated for 30 min (in a total volume of 60uL) at 37 °C with dilutions of purified immunoglobulin from the sera from FILORAB3 and control immunized mice in a 96-well U-bottom plate before infection of a monolayer of 293T target cells seeded in a 96-well flat bottom plate 24 h prior in 5% complete DMEM. At 48 h after incubation at 37 °C, the target cells were lysed and spin clarified, and supernatant from these cells was measured for luciferase activity (in relative light units) by FluoStar Omega fluorimeter in a luciferase assay based in 96-well white plates using D-luciferin salt (Sigma) reconstituted in ATP-containing buffer to a concentration of 0.5mM as the substrate. Positive luciferase activity indicated infectivity by pseudotyped virus, and the infectivity was normalized to the infectivity in control conditions where no antibody was added (i.e., maximum infectivity signal). Neutralization was reported as a percentage of infectivity, and potent neutralization activity was measured by IC50 values.

Acknowledgments

This work was also funded in part through the NIAID Division of Intramural Research and the NIAID Division of Clinical Research, Battelle Memorial Institute's prime contract with the U.S. National Institute of Allergy and Infectious Diseases (NIAID) under Contract No. HHSN272200700016I. K.R.H. performed this work as an employee of Battelle Memorial Institute. We thank Oscar Rojas, Isis Alexander, and Kristina Howard (Integrated Research Facility, NIH, Fort Detrick, MD) for hands-on animal work and management.

We thank Jennifer Wilson (Thomas Jefferson University, Philadelphia, PA) for critical reading and editing of the manuscript and Jiro Wada for help with the preparations of the illustrations.

R.F.J. and M.J.S are inventors on the U.S. Provisional Patent Application Title: "Multivalent vaccines for rabies virus and filoviruses". M.J.S. serves on the Scientific Advisory Board of IDT Biologika, Dessau, Germany. All other authors declare no competing interests.

References

1. **Mühlberger E, Hensley, Lisa, Towner, Jonathan.** 2017. Current Topics in Microbiology and Immunology doi:10.1007/978-3-319-68948-7.
2. **Kuhn JH.** 2017. Guide to the Correct Use of Filoviral Nomenclature. Curr Top Microbiol Immunol **411:**447-460.
3. **Keshwara R, Johnson RF, Schnell MJ.** 2017. Toward an Effective Ebola Virus Vaccine. Annu Rev Med **68:**371-386.
4. **Organization WH.** 12 February 2018. Ebola virus disease. http://www.who.int/news-room/fact-sheets/detail/ebola-virus-disease. Accessed
5. **Volchkov VE, Volchkova VA, Stroher U, Becker S, Dolnik O, Cieplik M, Garten W, Klenk HD, Feldmann H.** 2000. Proteolytic processing of Marburg virus glycoprotein. Virology **268:**1-6.
6. **Geyer H, Will C, Feldmann H, Klenk HD, Geyer R.** 1992. Carbohydrate structure of Marburg virus glycoprotein. Glycobiology **2:**299-312.
7. **Manicassamy B, Wang J, Rumschlag E, Tymen S, Volchkova V, Volchkov V, Rong L.** 2007. Characterization of Marburg virus glycoprotein in viral entry. Virology **358:**79-88.
8. **Geisbert TW, Hensley LE, Geisbert JB, Leung A, Johnson JC, Grolla A, Feldmann H.** 2010. Postexposure treatment of Marburg virus infection. Emerg Infect Dis **16:**1119-1122.
9. **Dye JM, Herbert AS, Kuehne AI, Barth JF, Muhammad MA, Zak SE, Ortiz RA, Prugar LI, Pratt WD.** 2012. Postexposure antibody prophylaxis protects nonhuman primates from filovirus disease. Proc Natl Acad Sci U S A **109:**5034-5039.
10. **Fusco ML, Hashiguchi T, Cassan R, Biggins JE, Murin CD, Warfield KL, Li S, Holtsberg FW, Shulenin S, Vu H, Olinger GG, Kim DH, Whaley KJ, Zeitlin L, Ward AB, Nykiforuk C, Aman MJ, Berry JD, Saphire EO.** 2015. Protective mAbs and Cross-Reactive mAbs Raised by Immunization with Engineered Marburg Virus GPs. PLoS Pathog **11:**e1005016.
11. **Mire CE, Geisbert JB, Borisevich V, Fenton KA, Agans KN, Flyak AI, Deer DJ, Steinkellner H, Bohorov O, Bohorova N, Goodman C, Hiatt A, Kim DH, Pauly MH, Velasco J, Whaley KJ, Crowe JE, Jr., Zeitlin L, Geisbert TW.** 2017. Therapeutic treatment of Marburg and Ravn virus infection in nonhuman primates with a human monoclonal antibody. Sci Transl Med **9**.
12. **Gsell PS, Camacho A, Kucharski AJ, Watson CH, Bagayoko A, Nadlaou SD, Dean NE, Diallo A, Diallo A, Honora DA, Doumbia M, Enwere G, Higgs ES, Mauget T, Mory D, Riveros X, Oumar FT, Fallah M, Toure A, Vicari AS, Longini IM, Edmunds WJ, Henao-Restrepo AM, Kieny MP, Keita S.** 2017. Ring vaccination with rVSV-ZEBOV under expanded access in response to an outbreak of Ebola virus disease in Guinea, 2016: an operational and vaccine safety report. Lancet Infect Dis **17:**1276-1284.
13. **Grant-Klein RJ, Van Deusen NM, Badger CV, Hannaman D, Dupuy LC, Schmaljohn CS.** 2012. A multiagent filovirus DNA vaccine delivered by intramuscular electroporation completely protects mice from ebola and Marburg virus challenge. Hum Vaccin Immunother **8:**1703-1706.
14. **Sarwar UN, Costner P, Enama ME, Berkowitz N, Hu Z, Hendel CS, Sitar S, Plummer S, Mulangu S, Bailer RT, Koup RA, Mascola JR, Nabel GJ, Sullivan NJ, Graham BS, Ledgerwood JE, Team VRCS.** 2015. Safety and immunogenicity of DNA vaccines encoding Ebolavirus and Marburgvirus wild-type glycoproteins in a phase I clinical trial. J Infect Dis **211:**549-557.
15. **Dye JM, Warfield KL, Wells JB, Unfer RC, Shulenin S, Vu H, Nichols DK, Aman MJ, Bavari S.** 2016. Virus-Like Particle Vaccination Protects Nonhuman Primates from Lethal Aerosol Exposure with Marburgvirus (VLP Vaccination Protects Macaques against Aerosol Challenges). Viruses **8:**94.

16. **Geisbert TW, Feldmann H.** 2011. Recombinant vesicular stomatitis virus-based vaccines against Ebola and Marburg virus infections. J Infect Dis **204 Suppl 3:**S1075-1081.
17. **Mire CE, Geisbert JB, Agans KN, Satterfield BA, Versteeg KM, Fritz EA, Feldmann H, Hensley LE, Geisbert TW.** 2014. Durability of a vesicular stomatitis virus-based marburg virus vaccine in nonhuman primates. PLoS One **9:**e94355.
18. **Jones SM, Feldmann H, Stroher U, Geisbert JB, Fernando L, Grolla A, Klenk HD, Sullivan NJ, Volchkov VE, Fritz EA, Daddario KM, Hensley LE, Jahrling PB, Geisbert TW.** 2005. Live attenuated recombinant vaccine protects nonhuman primates against Ebola and Marburg viruses. Nat Med **11:**786-790.
19. **Stonier SW, Herbert AS, Kuehne AI, Sobarzo A, Habibulin P, Dahan CVA, James RM, Egesa M, Cose S, Lutwama JJ, Lobel L, Dye JM.** 2017. Marburg virus survivor immune responses are Th1 skewed with limited neutralizing antibody responses. J Exp Med **214:**2563-2572.
20. **Arnon R, Ben-Yedidia T.** 2003. Old and new vaccine approaches. Int Immunopharmacol **3:**1195-1204.
21. **Natesan M, Jensen SM, Keasey SL, Kamata T, Kuehne AI, Stonier SW, Lutwama JJ, Lobel L, Dye JM, Ulrich RG.** 2016. Human Survivors of Disease Outbreaks Caused by Ebola or Marburg Virus Exhibit Cross-Reactive and Long-Lived Antibody Responses. Clin Vaccine Immunol **23:**717-724.
22. **Bukreyev A, Skiadopoulos MH, Murphy BR, Collins PL.** 2006. Nonsegmented negative-strand viruses as vaccine vectors. J Virol **80:**10293-10306.
23. **Dunkel A, Shen S, LaBranche CC, Montefiori D, McGettigan JP.** 2015. A Bivalent, Chimeric Rabies Virus Expressing Simian Immunodeficiency Virus Envelope Induces Multifunctional Antibody Responses. AIDS Res Hum Retroviruses **31:**1126-1138.
24. **Liu Q, Fan C, Li Q, Zhou S, Huang W, Wang L, Sun C, Wang M, Wu X, Ma J, Li B, Xie L, Wang Y.** 2017. Antibody-dependent-cellular-cytotoxicity-inducing antibodies significantly affect the post-exposure treatment of Ebola virus infection. Sci Rep **7:**45552.
25. **Shedlock DJ, Bailey MA, Popernack PM, Cunningham JM, Burton DR, Sullivan NJ.** 2010. Antibody-mediated neutralization of Ebola virus can occur by two distinct mechanisms. Virology **401:**228-235.
26. **Corti D, Misasi J, Mulangu S, Stanley DA, Kanekiyo M, Wollen S, Ploquin A, Doria-Rose NA, Staupe RP, Bailey M, Shi W, Choe M, Marcus H, Thompson EA, Cagigi A, Silacci C, Fernandez-Rodriguez B, Perez L, Sallusto F, Vanzetta F, Agatic G, Cameroni E, Kisalu N, Gordon I, Ledgerwood JE, Mascola JR, Graham BS, Muyembe-Tamfun JJ, Trefry JC, Lanzavecchia A, Sullivan NJ.** 2016. Protective monotherapy against lethal Ebola virus infection by a potently neutralizing antibody. Science **351:**1339-1342.
27. **Nimmerjahn F, Gordan S, Lux A.** 2015. FcgammaR dependent mechanisms of cytotoxic, agonistic, and neutralizing antibody activities. Trends Immunol **36:**325-336.
28. **He W, Chen CJ, Mullarkey CE, Hamilton JR, Wong CK, Leon PE, Uccellini MB, Chromikova V, Henry C, Hoffman KW, Lim JK, Wilson PC, Miller MS, Krammer F, Palese P, Tan GS.** 2017. Alveolar macrophages are critical for broadly-reactive antibody-mediated protection against influenza A virus in mice. Nat Commun **8:**846.
29. **Yamada DH, Elsaesser H, Lux A, Timmerman JM, Morrison SL, de la Torre JC, Nimmerjahn F, Brooks DG.** 2015. Suppression of Fcgamma-receptor-mediated antibody effector function during persistent viral infection. Immunity **42:**379-390.
30. **Bournazos S, Ravetch JV.** 2017. Fcgamma Receptor Function and the Design of Vaccination Strategies. Immunity **47:**224-233.
31. **Fisher CR, Streicker DG, Schnell MJ.** 2018. The spread and evolution of rabies virus: conquering new frontiers. Nat Rev Microbiol **16:**241-255.

32. **Conzelmann KK, Schnell M.** 1994. Rescue of synthetic genomic RNA analogs of rabies virus by plasmid-encoded proteins. J Virol **68:**713-719.
33. **Schnell MJ, Mebatsion T, Conzelmann KK.** 1994. Infectious rabies viruses from cloned cDNA. EMBO J **13:**4195-4203.
34. **Mebatsion T, Schnell MJ, Cox JH, Finke S, Conzelmann KK.** 1996. Highly stable expression of a foreign gene from rabies virus vectors. Proc Natl Acad Sci U S A **93:**7310-7314.
35. **Johnson RF, Kurup D, Hagen KR, Fisher C, Keshwara R, Papaneri A, Perry DL, Cooper K, Jahrling PB, Wang JT, Ter Meulen J, Wirblich C, Schnell MJ.** 2016. An Inactivated Rabies Virus-Based Ebola Vaccine, FILORAB1, Adjuvanted With Glucopyranosyl Lipid A in Stable Emulsion Confers Complete Protection in Nonhuman Primate Challenge Models. J Infect Dis **214:**S342-S354.
36. **Kurup D, Wirblich C, Feldmann H, Marzi A, Schnell MJ.** 2015. Rhabdovirus-based vaccine platforms against henipaviruses. J Virol **89:**144-154.
37. **Papaneri AB, Wirblich C, Cooper K, Jahrling PB, Schnell MJ, Blaney JE.** 2012. Further characterization of the immune response in mice to inactivated and live rabies vaccines expressing Ebola virus glycoprotein. Vaccine **30:**6136-6141.
38. **Perrin P, Morgeaux S.** 1995. Inactivation of DNA by beta-propiolactone. Biologicals **23:**207-211.
39. **Mohan GS, Ye L, Li W, Monteiro A, Lin X, Sapkota B, Pollack BP, Compans RW, Yang C.** 2015. Less is more: Ebola virus surface glycoprotein expression levels regulate virus production and infectivity. J Virol **89:**1205-1217.
40. **Mittler E, Kolesnikova L, Hartlieb B, Davey R, Becker S.** 2011. The cytoplasmic domain of Marburg virus GP modulates early steps of viral infection. J Virol **85:**8188-8196.
41. **Blaney JE, Wirblich C, Papaneri AB, Johnson RF, Myers CJ, Juelich TL, Holbrook MR, Freiberg AN, Bernbaum JG, Jahrling PB, Paragas J, Schnell MJ.** 2011. Inactivated or live-attenuated bivalent vaccines that confer protection against rabies and Ebola viruses. J Virol **85:**10605-10616.
42. **Warfield KL, Alves DA, Bradfute SB, Reed DK, VanTongeren S, Kalina WV, Olinger GG, Bavari S.** 2007. Development of a model for marburgvirus based on severe-combined immunodeficiency mice. Virol J **4:**108.
43. **Takai T, Li M, Sylvestre D, Clynes R, Ravetch JV.** 1994. FcR gamma chain deletion results in pleiotrophic effector cell defects. Cell **76:**519-529.
44. **Ackerman ME, Alter G.** 2013. Opportunities to exploit non-neutralizing HIV-specific antibody activity. Curr HIV Res **11:**365-377.
45. **Willet M, Kurup D, Papaneri A, Wirblich C, Hooper JW, Kwilas SA, Keshwara R, Hudacek A, Beilfuss S, Rudolph G, Pommerening E, Vos A, Neubert A, Jahrling P, Blaney JE, Johnson RF, Schnell MJ.** 2015. Preclinical Development of Inactivated Rabies Virus-Based Polyvalent Vaccine Against Rabies and Filoviruses. J Infect Dis **212 Suppl 2:**S414-424.
46. **Clegg CH, Roque R, Perrone LA, Rininger JA, Bowen R, Reed SG.** 2014. GLA-AF, an emulsion-free vaccine adjuvant for pandemic influenza. PLoS One **9:**e88979.
47. **Arias MA, Van Roey GA, Tregoning JS, Moutaftsi M, Coler RN, Windish HP, Reed SG, Carter D, Shattock RJ.** 2012. Glucopyranosyl Lipid Adjuvant (GLA), a Synthetic TLR4 agonist, promotes potent systemic and mucosal responses to intranasal immunization with HIVgp140. PLoS One **7:**e41144.
48. **Coler RN, Baldwin SL, Shaverdian N, Bertholet S, Reed SJ, Raman VS, Lu X, DeVos J, Hancock K, Katz JM, Vedvick TS, Duthie MS, Clegg CH, Van Hoeven N, Reed SG.** 2010. A synthetic adjuvant to enhance and expand immune responses to influenza vaccines. PLoS One **5:**e13677.
49. **Organization WH.** 2007. Rabies vaccines WHO position paper. http://www.who.int/wer/2007/wer8249_50.pdf. Accessed

50. **Kishishita N, Takeda N, Anuegoonpipat apreecha S.** 2013. Development of a pseudotyped-lentiviral-vector-based ne n assay for chikungunya virus infection. J Clin Microbiol **51:**1389-1395.

51. **Montefiori DC.** 2009. Measuring HIV ne n in a luciferase reporter gene assay. Methods Mol Biol **485:**395-405.

52. **Flyak AI, Ilinykh PA, Murin CD, Garron Fusco ML, Hashiguchi T, Bornholdt ZA, Slaughter JC, Sapparapu G, Klages C, K Ward AB, Saphire EO, Bukreyev A, Crowe JE, Jr.** 2015. Mechanism of human antibod d neutralization of Marburg virus. Cell **160:**893-903.

53. **Moore SM, Hanlon CA.** 2010. Rabies-sp bodies: measuring surrogates of protection against a fatal disease. PLoS Negl Trop I .

54. **McGettigan JP.** 2010. Experimental rab es for humans. Expert Rev Vaccines **9:**1177-1186.

55. **Faul EJ, Aye PP, Papaneri AB, Pahar B, n JP, Schiro F, Chervoneva I, Montefiori DC, Lackner AA, Schnell MJ.** 2009. Rabies v vaccines elicit neutralizing antibodies, poly-functional CD8+ T cell, and protect rhes ues from AIDS-like disease after SIV(mac251) challenge. Vaccine **28:**299-308.

56. **Blaney JE, Marzi A, Willet M, Papaneri ich C, Feldmann F, Holbrook M, Jahrling P, Feldmann H, Schnell MJ.** 2013. Antiboc and protection from lethal Ebola virus challenge in nonhuman primates immu rabies virus based bivalent vaccine. PLoS Pathog **9:**e1003389.

57. **Kajihara M, Marzi A, Nakayama E, Nod la M, Manzoor R, Matsuno K, Feldmann H, Yoshida R, Kawaoka Y, Takada A.** 2012 n of Marburg virus budding by nonneutralizing antibodies to the envelope glycoprotein **5:**13467-13474.

58. **Smith P, DiLillo DJ, Bournazos S, Li F, R** 2012. Mouse model recapitulating human Fcgamma receptor structural and funct sity. Proc Natl Acad Sci U S A **109:**6181-6186.

59. **Bruhns P.** 2012. Properties of mouse ar IgG receptors and their contribution to disease models. Blood **119:**5640-5649.

60. **Matrajt L, Britton T, Halloran ME, Long** 2015. One versus two doses: What is the best use of vaccine in an influenza pandemic cs **13:**17-27.

61. **Kosuwon P, Sutra S, Kosalaraksa P.** 20(age of a two-dose versus one-dose varicella vaccine in healthy non-immune teenagers and young adults. Southeast Asian J Trop Med Public Health **35:**697-701.

62. **Bernard KW, Roberts MA, Sumner J, Winkler WG, Mallonee J, Baer GM, Chaney R.** 1982. Human diploid cell rabies vaccine. Effectiveness of immunization with small intradermal or subcutaneous doses. JAMA **247:**1138-1142.

63. **Toellner KM, Sze DM, Zhang Y.** 2018. What Are the Primary Limitations in B-Cell Affinity Maturation, and How Much Affinity Maturation Can We Drive with Vaccination? A Role for Antibody Feedback. Cold Spring Harb Perspect Biol **10**.

64. **Publicover J, Ramsburg E, Rose JK.** 2004. Characterization of nonpathogenic, live, viral vaccine vectors inducing potent cellular immune responses. J Virol **78:**9317-9324.

65. **de Vries RD, Rimmelzwaan GF.** 2016. Viral vector-based influenza vaccines. Hum Vaccin Immunother **12:**2881-2901.

66. **Howell KA, Brannan JM, Bryan C, McNeal A, Davidson E, Turner HL, Vu H, Shulenin S, He S, Kuehne A, Herbert AS, Qiu X, Doranz BJ, Holtsberg FW, Ward AB, Dye JM, Aman MJ.** 2017. Cooperativity Enables Non-neutralizing Antibodies to Neutralize Ebolavirus. Cell Rep **19:**413-424.

67. **Qiu X, Wong G, Audet J, Bello A, Fernando L, Alimonti JB, Fausther-Bovendo H, Wei H, Aviles J, Hiatt E, Johnson A, Morton J, Swope K, Bohorov O, Bohorova N, Goodman C, Kim D, Pauly MH,**

Velasco J, Pettitt J, Olinger GG, Whaley K, Xu B, Strong JE, Zeitlin L, Kobinger GP. 2014. Reversion of advanced Ebola virus disease in nonhuman primates with ZMapp. Nature **514:**47-53.

68. **Hangartner L, Zellweger RM, Giobbi M, Weber J, Eschli B, McCoy KD, Harris N, Recher M, Zinkernagel RM, Hengartner H.** 2006. Nonneutralizing antibodies binding to the surface glycoprotein of lymphocytic choriomeningitis virus reduce early virus spread. J Exp Med **203:**2033-2042.

69. **Holl V, Peressin M, Decoville T, Schmidt S, Zolla-Pazner S, Aubertin AM, Moog C.** 2006. Nonneutralizing antibodies are able to inhibit human immunodeficiency virus type 1 replication in macrophages and immature dendritic cells. J Virol **80:**6177-6181.

70. **Holl V, Peressin M, Moog C.** 2009. Antibody-Mediated Fcgamma Receptor-Based Mechanisms of HIV Inhibition: Recent Findings and New Vaccination Strategies. Viruses **1:**1265-1294.

71. **Excler JL, Ake J, Robb ML, Kim JH, Plotkin SA.** 2014. Nonneutralizing functional antibodies: a new "old" paradigm for HIV vaccines. Clin Vaccine Immunol **21:**1023-1036.

72. **Zolla-Pazner S.** 2016. Non-neutralizing antibody functions for protection and control HIV in humans and SIV and SHIV in non-human primates. AIDS **30:**2551-2553.

73. **Singh K, Marasini B, Chen X, Spearman P.** 2018. A novel Ebola virus antibody-dependent cell-mediated cytotoxicity (Ebola ADCC) assay. J Immunol Methods **460:**10-16.

74. **Terajima M, Cruz J, Co MD, Lee JH, Kaur K, Wrammert J, Wilson PC, Ennis FA.** 2011. Complement-dependent lysis of influenza a virus-infected cells by broadly cross-reactive human monoclonal antibodies. J Virol **85:**13463-13467.

75. **Rattan A, Pawar SD, Nawadkar R, Kulkarni N, Lal G, Mullick J, Sahu A.** 2017. Synergy between the classical and alternative pathways of complement is essential for conferring effective protection against the pandemic influenza A(H1N1) 2009 virus infection. PLoS Pathog **13:**e1006248.

76. **O'Brien KB, Morrison TE, Dundore DY, Heise MT, Schultz-Cherry S.** 2011. A protective role for complement C3 protein during pandemic 2009 H1N1 and H5N1 influenza A virus infection. PLoS One **6:**e17377.

77. **Lilienthal GM, Rahmoller J, Petry J, Bartsch YC, Leliavski A, Ehlers M.** 2018. Potential of Murine IgG1 and Human IgG4 to Inhibit the Classical Complement and Fcgamma Receptor Activation Pathways. Front Immunol **9:**958.

78. **Stoiber H, Clivio A, Dierich MP.** 1997. Role of complement in HIV infection. Annu Rev Immunol **15:**649-674.

79. **Xu Y, Zhang C, Jia L, Wen C, Liu H, Wang Y, Sun Y, Huang L, Zhou Y, Song H.** 2009. A novel approach to inhibit HIV-1 infection and enhance lysis of HIV by a targeted activator of complement. Virol J **6:**123.

80. **Dubois Cauwelaert N, Desbien AL, Hudson TE, Pine SO, Reed SG, Coler RN, Orr MT.** 2016. The TLR4 Agonist Vaccine Adjuvant, GLA-SE, Requires Canonical and Atypical Mechanisms of Action for TH1 Induction. PLoS One **11:**e0146372.

81. **Orr MT, Desbien AL, Cauwelaert ND, Reed SG.** 2016. Mechanisms of activity of the combination TLR4 agonist and emulsion adjuvant GLA-SE. The Journal of Immunology **196:**75.72-75.72.

82. **Daddario-DiCaprio KM, Geisbert TW, Geisbert JB, Stroher U, Hensley LE, Grolla A, Fritz EA, Feldmann F, Feldmann H, Jones SM.** 2006. Cross-protection against Marburg virus strains by using a live, attenuated recombinant vaccine. J Virol **80:**9659-9666.

83. **Alves DA, Glynn AR, Steele KE, Lackemeyer MG, Garza NL, Buck JG, Mech C, Reed DS.** 2010. Aerosol exposure to the angola strain of marburg virus causes lethal viral hemorrhagic Fever in cynomolgus macaques. Vet Pathol **47:**831-851.

84. **Cross RW, Fenton KA, Geisbert JB, Ebihara H, Mire CE, Geisbert TW.** 2015. Comparison of the Pathogenesis of the Angola and Ravn Strains of Marburg Virus in the Outbred Guinea Pig Model. J Infect Dis **212 Suppl 2:**S258-270.

85. **Thi EP, Mire CE, Ursic-Bedoya R, Geisbert JB, Lee ACH, Agans KN, Robbins M, Deer DJ, Fenton KA, MacLachlan I, Geisbert TW.** 2014. Marburg virus infection in nonhuman primates: Therapeutic treatment by lipid-encapsulated siRNA. Sci Transl Med **6:**250ra116.

86. **Geisbert TW, Geisbert JB, Leung A, Daddario-DiCaprio KM, Hensley LE, Grolla A, Feldmann H.** 2009. Single-injection vaccine protects nonhuman primates against infection with marburg virus and three species of ebola virus. J Virol **83:**7296-7304.

87. **Towner JS, Khristova ML, Sealy TK, Vincent MJ, Erickson BR, Bawiec DA, Hartman AL, Comer JA, Zaki SR, Stroher U, Gomes da Silva F, del Castillo F, Rollin PE, Ksiazek TG, Nichol ST.** 2006. Marburgvirus genomics and association with a large hemorrhagic fever outbreak in Angola. J Virol **80:**6497-6516.

872 **Figure. 1. FILORAB3 vaccine constructs**. Schematic of RABV vaccine constructs expressing
873 codon-optimized Angola strain MARV GP (FILORAB3) used for immunizations. MARV GP is
874 inserted between the N and P genes of the negative sense RNA genome of RABV. The 333
875 mutation in RABV G that attenuates neurovirulence is depicted.

876

877 **Figure. 2. Growth kinetics of recombinant RABV/MARV (FILORAB3).** Multi-step growth
878 curve comparing the kinetics of live virus replication of FILORAB3 (red), parental RABV vaccine
879 vector (BNSP333, blue), and recombinant rabies expressing codon-optimized Ebola
880 glycoprotein (FILORAB1, green) in the recovery cell line (BSR cells). BSR cells were infected
881 with a multiplicity of infection of 0.1 and supernatant was collected at 0, 24, 48, 72, and 96 h.
882 Virus titers were measured by foci-forming assay (in Y axis) and plotted through time (X axis).

883

884 **Figure 3. Vaccine vector characterization**. (a) VERO CCL-81 cells were infected at a MOI of
885 0.1 with BNSP333 parental rabies vaccine virus or recombinant FILORAB3 for 48 h later before
886 surface immunostaining with monoclonal antibodies directed against RABV G (Green) and
887 MARV GP (Red). Yellow indicates an overlap in the expression of both glycoproteins. (b) [left
888 panel] 4ug each of purified inactivated FILORAB3 and control virions were loaded onto a
889 denaturing 10% SDS-PAGE gel and stained with SYPRO Ruby to visualize incorporated
890 proteins. Full-length codon-optimized MARV GP and soluble MARV GP (2ug) with
891 transmembrane and cytoplasmic domain deletion (used for antibody capture in ELISAs) are
892 indicated by the red box. FILORAB1 purified virions were included as a control for successful
893 foreign glycoprotein incorporation. Critical RABV proteins are indicated. [right] Confirmation of
894 MARV GP incorporation into purified FILORAB3 virions by Western blot analysis. 2ug of purified
895 inactivated FILORAB3 or control virions were loaded onto 10%SDS-PAGE gel and transferred

to a nitrocellulose membrane. The blot was probed with a cocktail of two mouse-derived monoclonal antibodies specific for either the GP1 or GP2 subunit of MARV GP. Lysates from VERO cells infected with MARV were used a positive control. As a negative control, mock infected or Lassa virus infected VERO cell lysate was used.

Figure 4. Pathogenicity *in vivo* of FILORAB3 (A) Survival in newborn BALB/c mice (n=8) intracranially challenged with escalating doses of live FILORAB3 compared to live parental rabies virus (BNSP) in blue. (B) Survival in adult SCID mice (n=8) challenged intramuscularly with 6 $\log_{10}$ ffu of either FILORAB3 (red line), BNSP as a positive control (blue line), or PBS as a negative control (gray line). The log-rank (Mantel-Cox) test was used for comparison of survival curves to assess significant differences in survival.

Figure 5. Characterization of recombinant soluble MARV GP capture antigen for indirect ELISA. (a) 1ug of purified soluble MARV GP antigen was loaded onto a denaturing SDS-PAGE gel for Western Blot analysis. Blots were probed with anti-MARV GP1 or anti-MARV GP2 mouse monoclonal antibodies to confirm the presence of both subunits of MARV GP. (b) 50ng of soluble MARV GP antigen was used to coat wells in a 96-well plate for an indirect ELISA to test reactivity against MARV GP specific sera or antibodies. A 1:500 starting dilution of sera from an NHP survivor of Marburg virus disease (blue solid line) and a 1:50 starting dilution of an anti-GP2 monoclonal mouse antibody (red solid line) was analyzed in a 3-fold serial dilution in the ELISA. Pooled pre-immune sera from naïve BALB/c mice and NHPs were used as negative controls (red & blue dotted lines, respectively).

Figure 6. Humoral response to FILORAB3. (a) Experimental timeline for immunization of C57BL/6 mice (n=5 per group). C57BL/6 mice were immunized IM in the gastrocnemius muscle with a total of 10μg each of either FILORAB3 or BNSP333 inactivated viral particles adjuvanted with 5ug of a TLR-4 agonist in 2% stable emulsion (GLA-SE). All mice were primed on Day 0 and boosted once on Day 28. (b). Sera from immunized mice at Day 42 post inoculation were diluted 1:50 and analyzed in a 3-fold serial dilution via indirect ELISA to test for relative quantities of both MARV GP-specific (top panel) and RABV G-specific (bottom panel) antibodies. OD490 values were compared to antigen-specific monoclonal antibody positive control samples (black starred lines). (c) EC50 values from total MARV (top) and RABV (bottom) IgG ELISA curves were analyzed. Statistical significance was performed using unpaired t-test with Welch's correction to compare FILORAB3 and BNSP333-immunized groups. Results are presented as mean values; *p<0.05, **p<0.01, ***p<0.001. (d) IgG2 and IgG1 isotype responses in FILORAB3- and BNSP333-immunized mice were assessed by ELISA at Day 42 post inoculation to evaluate Th1 vs Th2 biased humoral immunity. (e) Purified IgG derived from pooled sera of FILORAB3 or BNSP333-immunized mice were analyzed in an *in vitro* pseudotyped lentivirus luciferase assay to determine the titers of MARV GP and RABV G neutralizing antibodies compared to a positive control monoclonal antibody known to neutralize either MARV or RABV pseudotyped virus *in vitro* (gray lines). Graphs are representative of average data from three independent experiments. Gray horizontal line indicates the threshold for 50% reduction in infection.

Figure 7. Murine MARV challenge model. (a) Experimental timeline for immunization of BALB/c mice and table of immunization groups included in the study. Groups of mice (n=10 per group) were immunized IM in the gastrocnemius muscle with the indicated treatments. Mice receiving 3 doses of adjuvanted inactivated vaccine (Group 7) were primed 61 days before challenge (D-61) and boosted both 54 and 40 days before challenge (D-54, D-40). Mice

receiving 2 doses of adjuvanted inactivated vaccine (Group 6) were primed 54 days before challenge (D-54) and boosted 40 days before challenge (D-40). All other groups of mice were primed 40 days before challenge (D-40). (b) Survival of BALB/c mice challenged intraperitoneally (i.p.) with a lethal dose of ma-MARV (1000pfu). (c) Pre-challenge humoral response in pooled mouse sera from each vaccine group after completion of immunization schedule (Day 0). Left and right panels show MARV GP and RABV-G specific antibody titers (ELISA curves and corresponding bar graph of EC50 values) compared to positive control monoclonal antibodies (gray lines, gray bars). (d) Bar graph of MARV GP-specific IgG1 and IgG2 isotype ELISA OD490 readings at the lowest antibody dilution (1:50) in pre-challenge sera (D0) for each vaccine group. (e) Post-challenge humoral response in pooled sera from survivor mice in the indicated vaccine groups after challenge with ma-MARV (Day 28, necropsy). Left and right panels show MARV GP and RABV-G specific antibody titers (Bar graph of EC50 values) compared to positive control monoclonal antibodies (gray bars). The D'Agostino & Pearson normality test was performed to test for normal distribution in each data set. Statistical significance for MARV-GP antibody titers was performed using the nonparametric Kruskal-Wallis test and Dunn's multiple comparisons test. For RABV G antibody titers, statistical significance was performed using ordinary one-way ANOVA with Holm-Sidak's multiple comparisons test. *$p<0.05$, **$p<0.01$, ***$p<0.001$, ****$p<0.0001$. (f) Bar graph of MARV GP-specific IgG1 and IgG2 isotype ELISA OD490 readings at the lowest antibody dilution (1:150) in post-challenge sera (D28) for each vaccine group. (g) Purified IgG derived from pooled mouse sera from the indicated vaccine groups were analyzed in an *in vitro* pseudotyped lentivirus luciferase assay to determine the titers of both pre-challenge (D0) and post-challenge (D28) MARV GP and RABV G neutralizing antibodies compared to a positive control monoclonal antibody known to neutralize either MARV or RABV pseudotyped virus *in vitro* (gray lines). Graphs are representative of average data from three independent experiments. Gray horizontal line indicates the threshold for 50% reduction in infection.

970

971 **Figure 8. Evaluation of NK cell-mediated antibody-dependent cellular cytotoxicity (ADCC)**
972 **effector function in an *in vitro* killing assay.** Purified IgG derived from pooled sera of BALB/c
973 mice immunized with either adjuvanted FILORAB3 (purple) or adjuvanted BNSP333 (blue) was
974 incubated with 3T3-MARV cells with or without addition of an antibody cocktail to block FcγRIII
975 receptor on the surface of NK cells. NK effector cells were subsequently added at an effector to
976 target cell ratio of 5:1. Killing was measured by flow cytometry (reported as % cytotoxicity). As
977 negative controls, 3T3-MARV cells were incubated with purified IgG alone in the absence of NK
978 effector cells (black/brown bars) or with NK effector cells alone and no antibodies (orange bars).
979 Statistical significance was performed using 2way ANOVA and post-hoc analysis with Tukey's
980 multiple comparisons test. *p<0.05, **p<0.01, ***p<0.001, ****p<0.0001. Data is representative
981 of average values from triplicate values across 3 independent experiments.

982

983 **Figure 9**. **Characterization of *in vitro* NK cell-mediated ADCC assay** (a) Schematic depicting
984 the experimental procedure and corresponding biological events for our *in vitro* mouse ADCC
985 direct killing assay. (b) [left panel] MARV GP expression in transduced mouse 3T3 target cells
986 was confirmed by flow cytometry (green curve) using an anti-MARV GP mouse monoclonal
987 antibody (mAb 3E10). 3T3 target cells expressing a non-specific viral glycoprotein (LASV GPC)
988 were stained with mAb 3E10 and assayed as a negative control (blue curve). VERO CCL81
989 cells infected at an MOI of 0.1 for 48 hrs were fixed and stained with mAb 3E10 and assayed as
990 a positive control for MARV GP expression (red curve). [right panel] Bar graph derived from flow
991 cytometry plots showing the geometric mean of medium fluorescence intensity (MFI) for both
992 GFP and MARV GP. (c) Phenotypic characterization by flow cytometry on magnetically-purified
993 NK cells enriched from splenocytes of naïve BALB/c mice to determine the purity of NK cells in
994 the effector cell population for the ADCC assay. CD3 and NKp46 biomarkers were used to

identify the percentage of effector NK cells in the population. (d) Gating strategy on 3T3-MARV cells for ADCC assay. Percentage of cytotoxicity was determined by the percentage of GFP+/Propidium iodide (PI)+ cells in the total parental GFP+ cell population. Top row is a representative flow plot of killing in 3T3-MARV target cells incubated with negative control sera. Bottom row is a representative flow plot of killing in target cells incubated with purified IgG derived from pooled sera from BALB/c mice immunized with FILORAB3. (e) Overlapping PI histograms of 3T3-MARV (blue) and 3T3-LASV (red) cells incubated with FILORAB3 purified IgG (1:100) showing the difference in cytotoxicity. 40,000 target cells were used in the assay.

Figure 10. Evaluation of the *in vivo* relevance of Fcγ receptor in protection against ma-MARV in a murine challenge model. (a) Experimental timeline for immunization of BALB/c mice and table of the immunization groups included in the study. Groups of wildtype or Fcγ knockout mice (n=12 per group) were immunized IM in the gastrocnemius muscle with the indicated treatments. Mice receiving 2 doses of adjuvanted inactivated vaccine (Groups 6 & 7) were primed 61 days before challenge (D-61) and boosted both 54 and 40 days before challenge (D-54, D-40). All other groups of mice were primed 40 days before challenge (D-40). (b) Survival of BALB/c mice challenged intraperitoneally (i.p.) with a lethal dose of ma-MARV (1000pfu). Statistical significance was performed using Log-rank (Mantel-Cox) test for comparison of survival curves (*p<0.05, **p<0.01). (c) Pre-challenge humoral response in pooled mouse sera from each vaccine group after completion of immunization schedule (Day 0). Left and right panels show MARV GP and RABV-G specific antibody titers (Bar graph of EC50 values) compared to positive control monoclonal antibodies (gray bars). The D'Agostino & Pearson normality test was performed to test for normal distribution in each data set. Statistical significance for both MARV-GP and RABV G antibody titers was performed using the nonparametric Kruskal-Wallis test and Dunn's multiple comparisons test (*p<0.05, **p<0.01, ***p<0.001, ****p<0.0001) (d) Post-challenge humoral response in pooled sera from survivor

mice in the indicated vaccine groups after challenge with ma-MARV (Day 28, necropsy). [left & middle graphs] MARV GP and RABV G specific antibody titers are represented by EC50 values of ELISA curves compared to positive control monoclonal antibodies (gray bars). The D'Agostino & Pearson normality test was performed to test for normal distribution in each data set. Statistical significance for MARV-GP antibody titers was performed using the nonparametric Kruskal-Wallis test and Dunn's multiple comparisons test (*p<0.05, **p<0.01, ***p<0.001, ****p<0.0001). [right graph] Bar graph of MARV GP-specific IgG1 and IgG2 isotype ELISA OD490 readings at the lowest antibody dilution (1:50) in post-challenge sera (D28) for survivors in the indicated vaccine groups. (e) Pooled sera from mice from the indicated vaccine groups were analyzed in an *in vitro* pseudotyped lentivirus luciferase assay to determine the titers of both pre-challenge (D0) and post-challenge (D28) MARV GP and RABV G neutralizing antibodies compared to a positive control monoclonal antibody known to neutralize either MARV or RABV pseudotyped virus *in vitro* (gray lines). Graphs are representative of average data from three independent experiments. Gray horizontal line indicates the threshold for 50% reduction in infection.

Figure 1

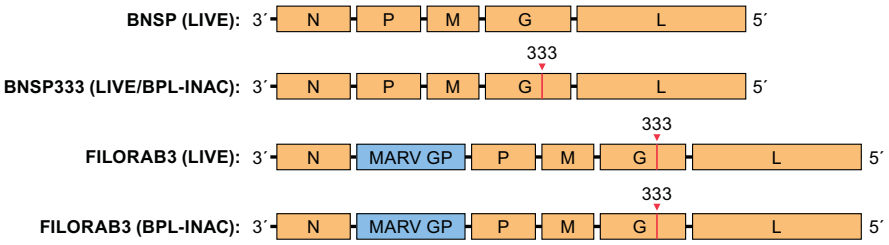

Figure 2

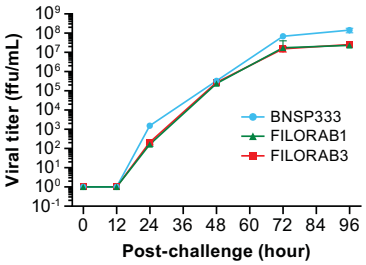

Figure 3

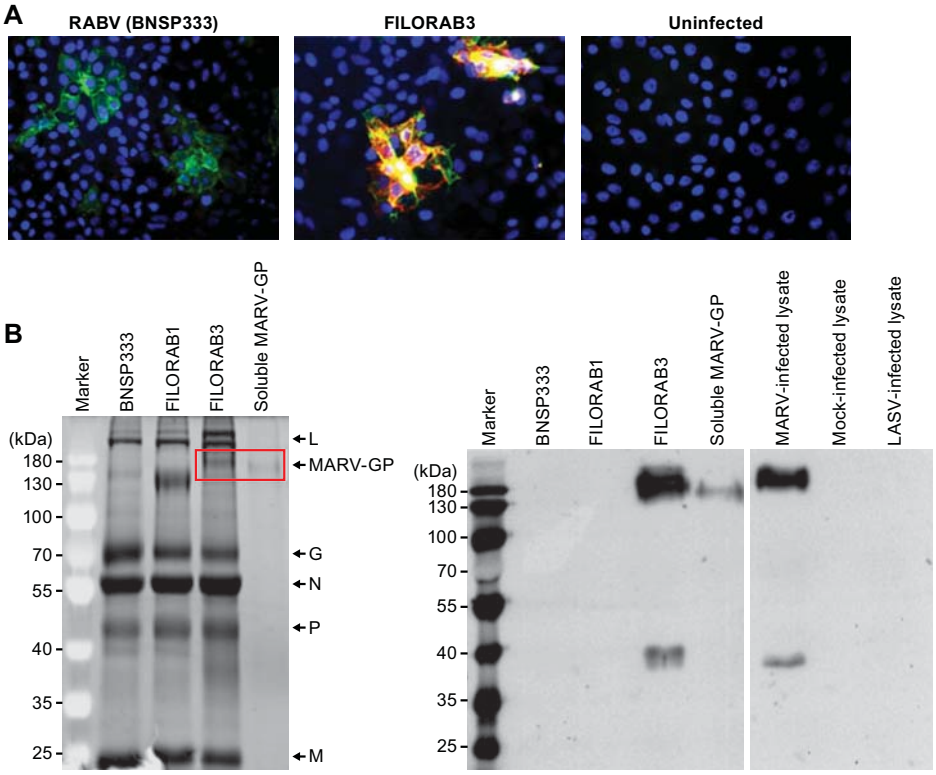

Figure 4

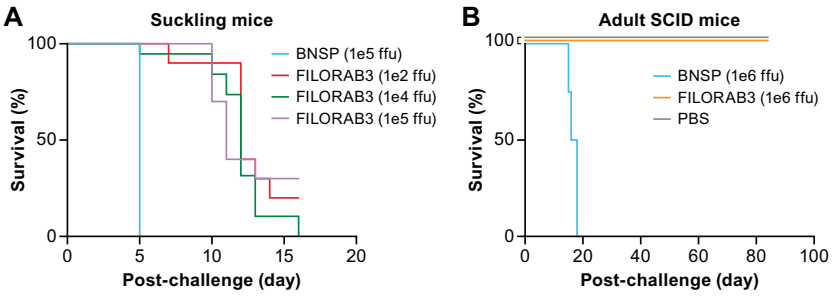

Figure 5

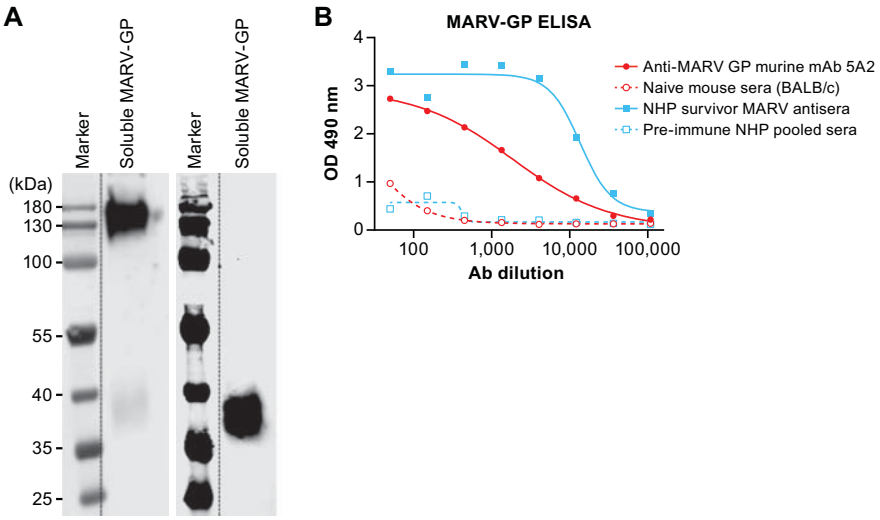

Figure 6

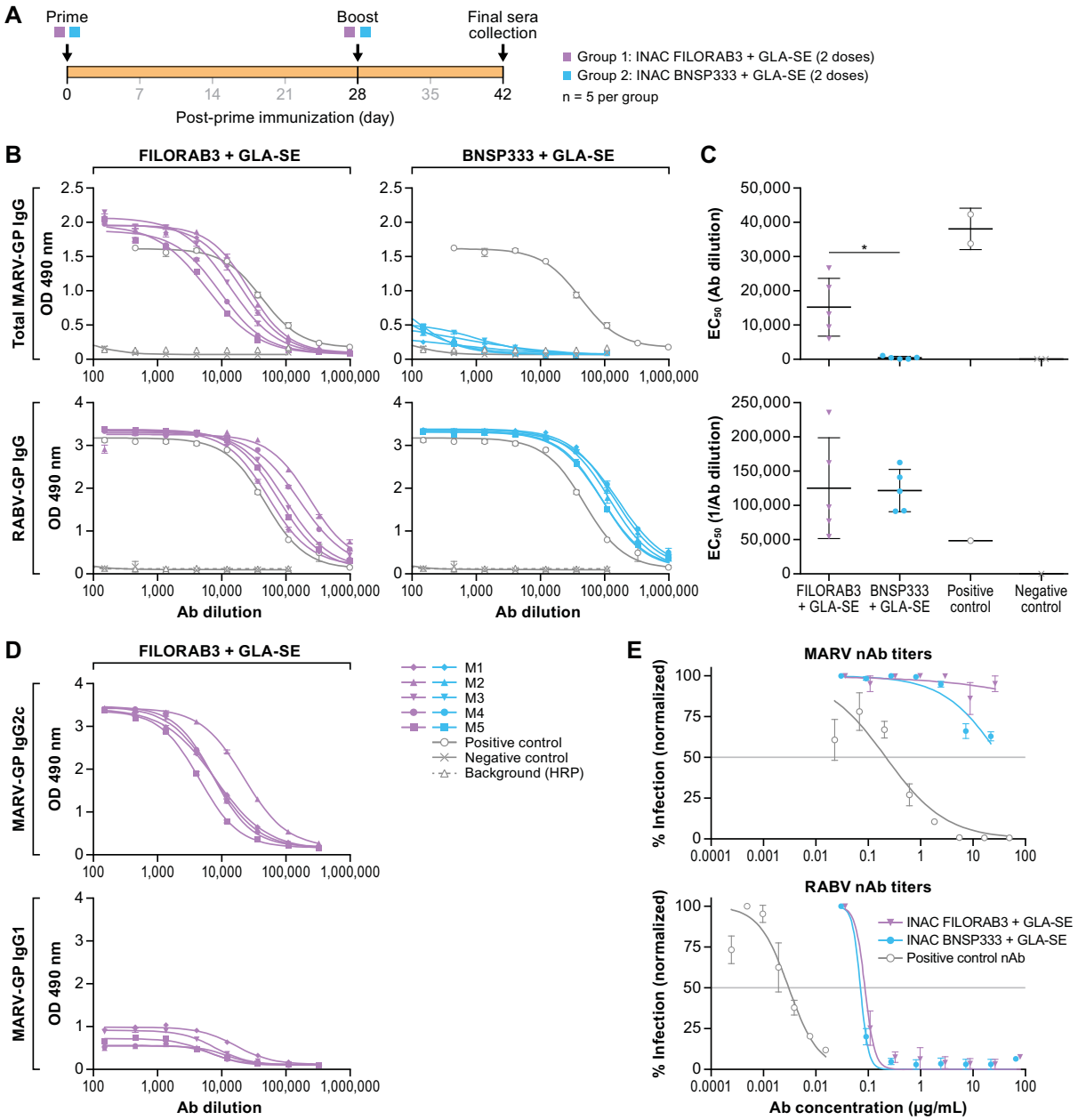

Figure 7

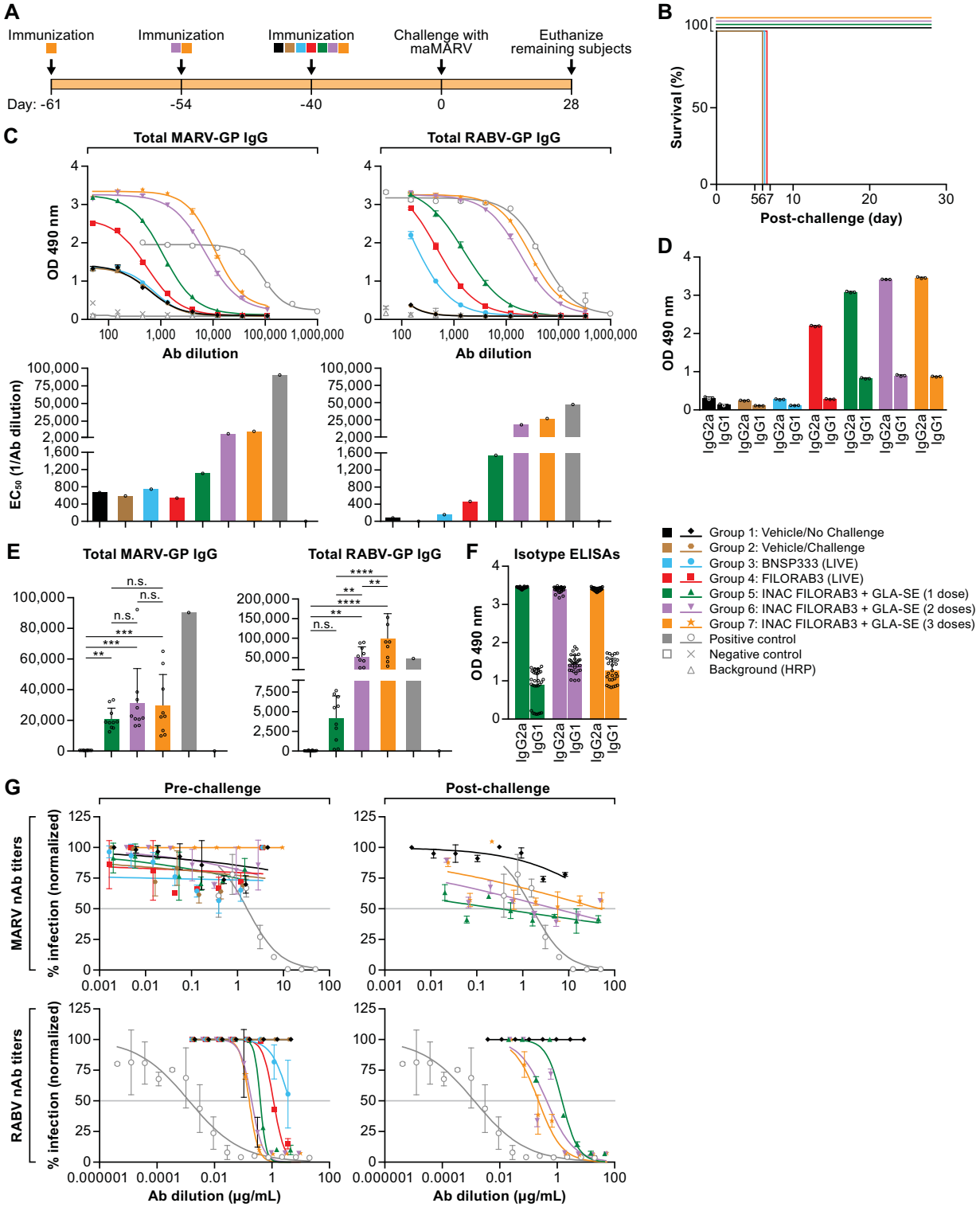

Figure 8

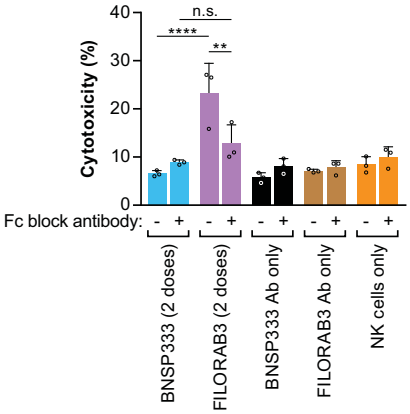

Figure 9

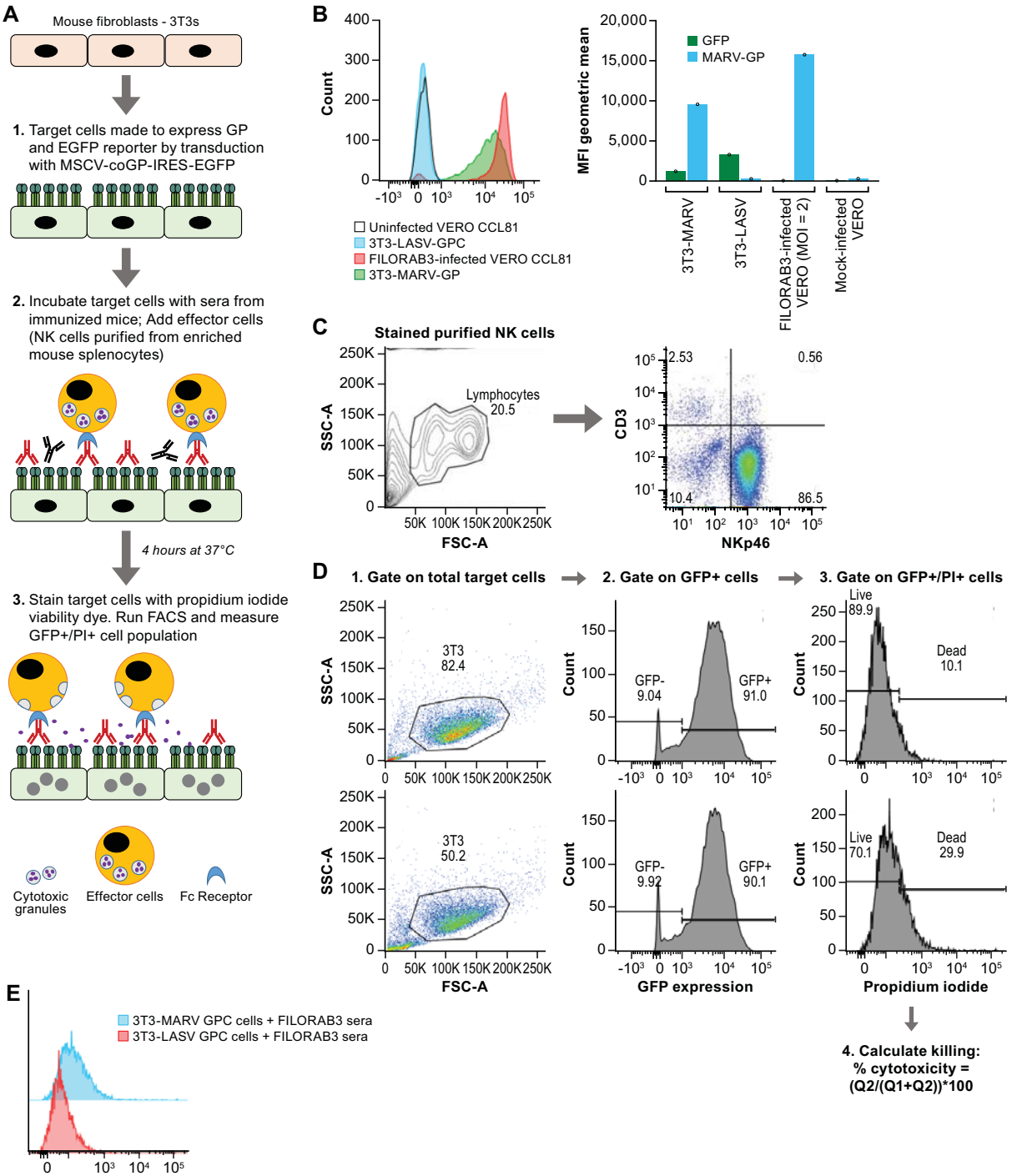

Figure 10